Natural Resources Canada / Ressources naturelles Canada

OPEN FILE 3497

NOTE:

Although every effort has been made to ensure accuracy, this Open File Report has not been edited for conformity with Geological Survey of Canada standards.

PALEOTEMPERATURE HISTORY OF THE PEACE RIVER ARCH REGION: CONSTRAINTS FROM APATITE FISSION TRACK ANALYSIS (Panel 2 of 2)

Dale R. Issler[1], Sean D. Willett[2], Christopher Beaumont[3], Raymond A. Donelick[4], and Alexander M. Grist[3]

[1]Geological Survey of Canada, Calgary, AB, [2]Pennsylvania State University, PA, [3]Dalhousie University, Halifax, NS and [4]Donelick Analytical, Katy, TX

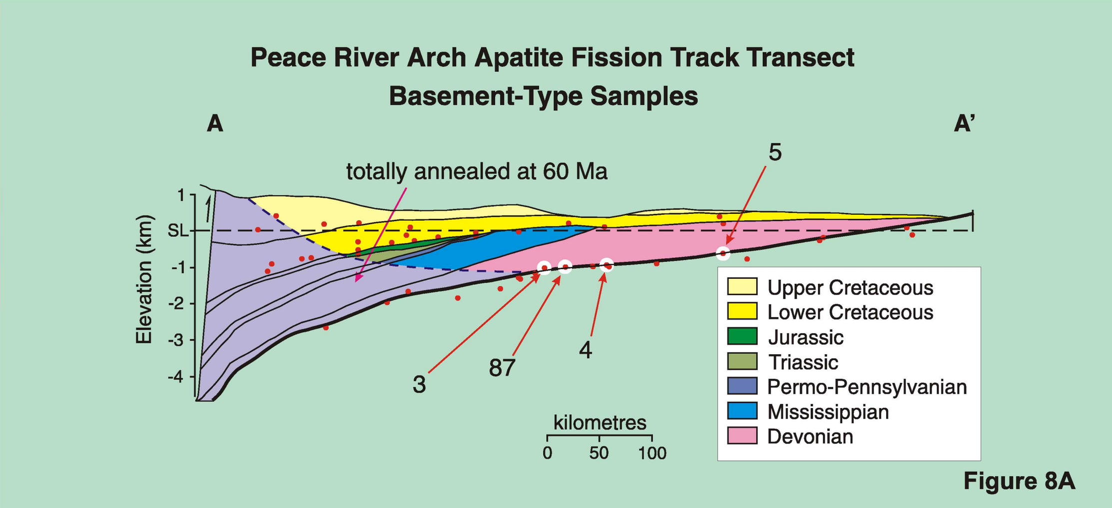

Figure 8A

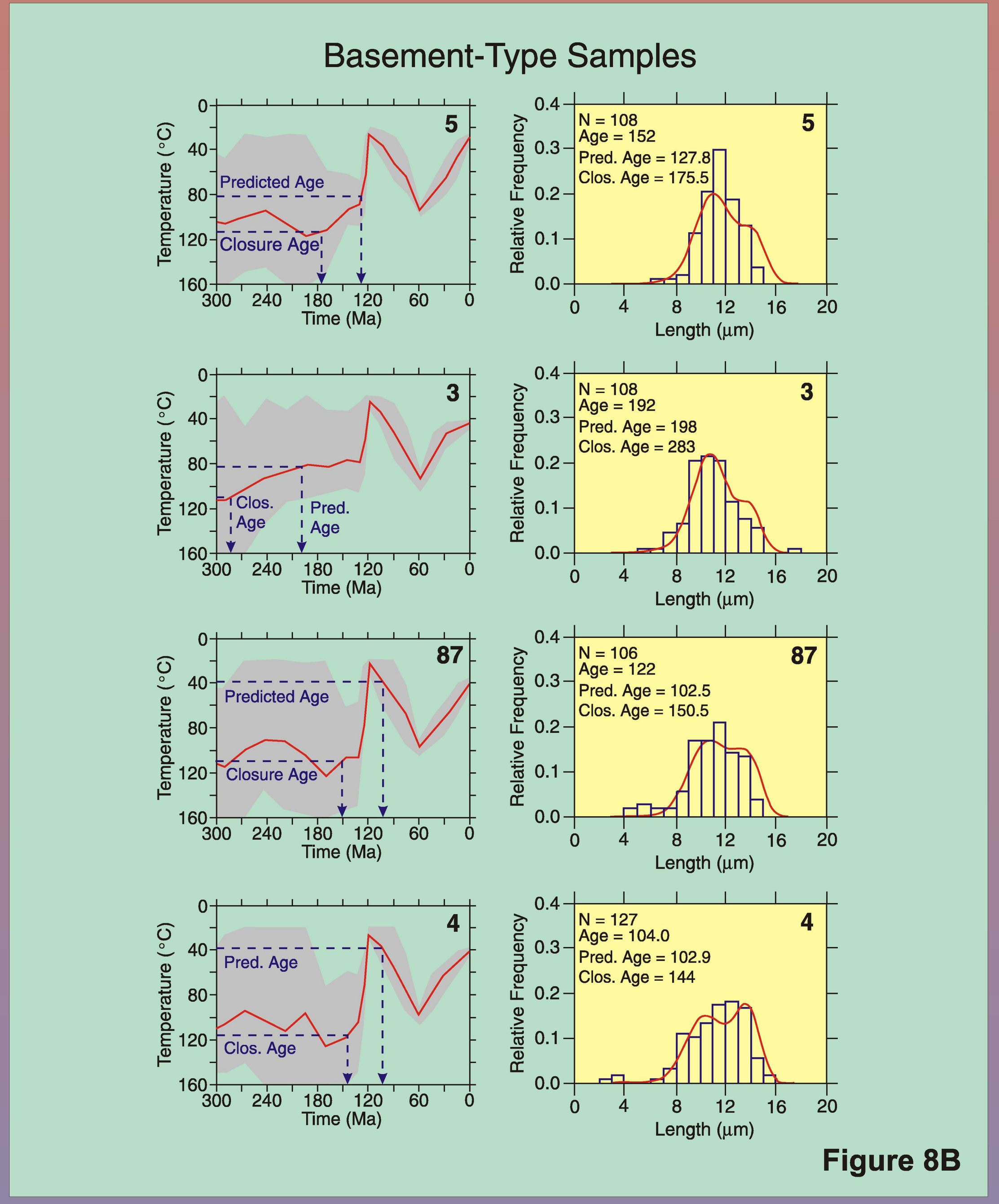

Figure 8B

Figure 8. A) Location for examples of basement-type PRA apatite fission track samples. B) Inferred temperature histories (left column) and predicted and measured AFT ages and track length distributions (right column) for basement-type samples. Mean temperature history (red curve) is shown with corresponding bounds on acceptable solutions (grey area); calculated track length distribution corresponding to the mean thermal history is shown superimposed on the measured track length distribution (histogram). Basement-type samples have experienced multiple phases of heating and cooling corresponding to deposition and erosion of a Paleozoic shelf sequence and deposition and erosion of a Mesozoic-Cenozoic foreland basin sequence. The pre-Cretaceous thermal history is poorly resolved due to thermal overprinting by foreland basin deposition. However, using 60 Ma as a model constraint on the time of maximum Cenozoic temperature, we can better resolve the magnitude of the most recent heating event. Thermal histories were constrained to increase in temperature from 120 Ma to 60 Ma and decrease in temperature from 60 Ma to the current temperature. Temperature at 120 Ma was constrained to be <40°C, reflecting the thin Paleozoic cover remaining at this time. To avoid unreasonable flucuations in temperature, thermal histories were not allowed to change more rapidly than 5°C/m.y. prior to 120 Ma but otherwise remain unconstrained.

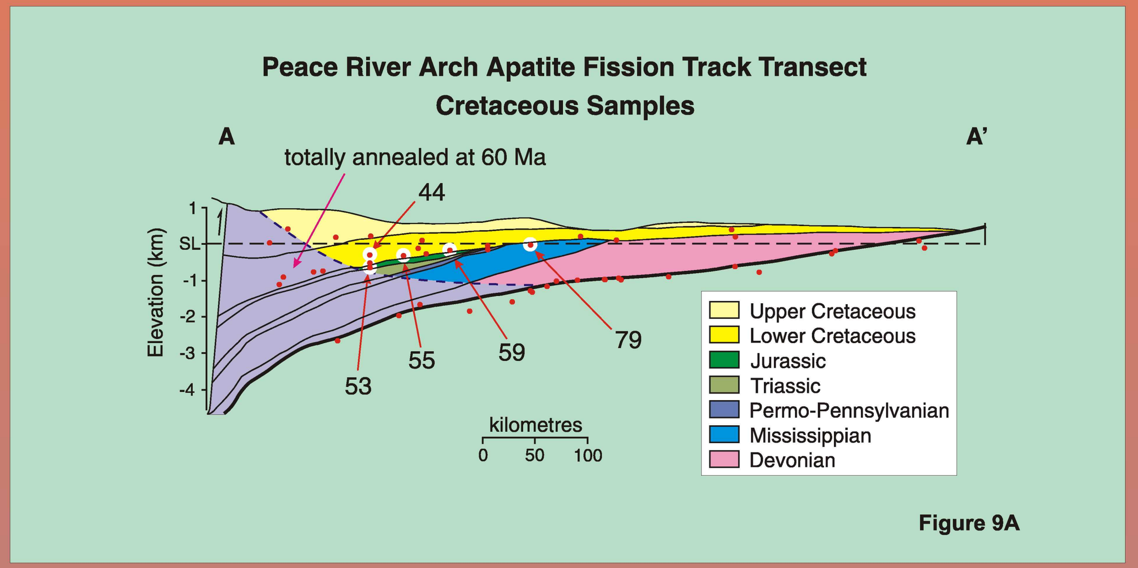

Figure 9A

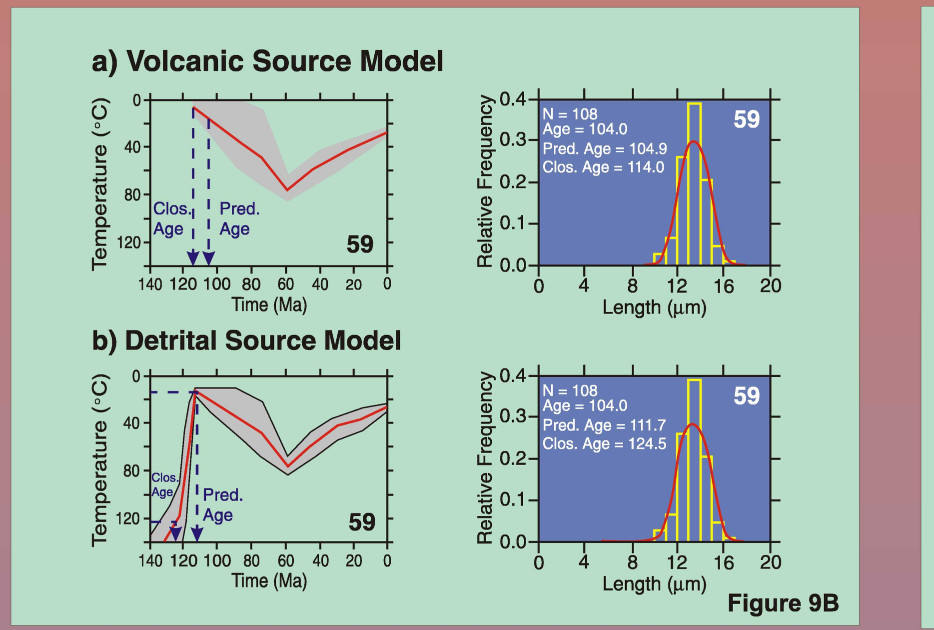

Figure 9B

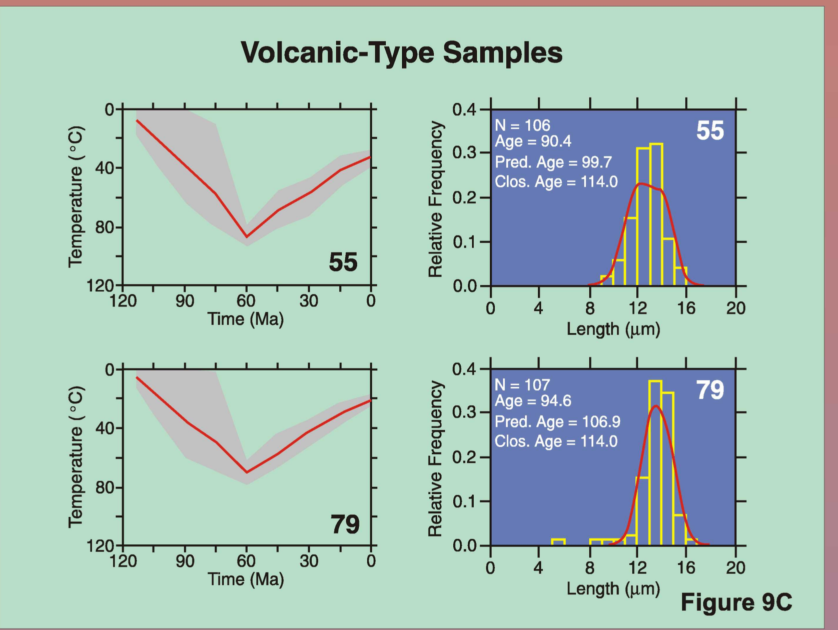

Figure 9C

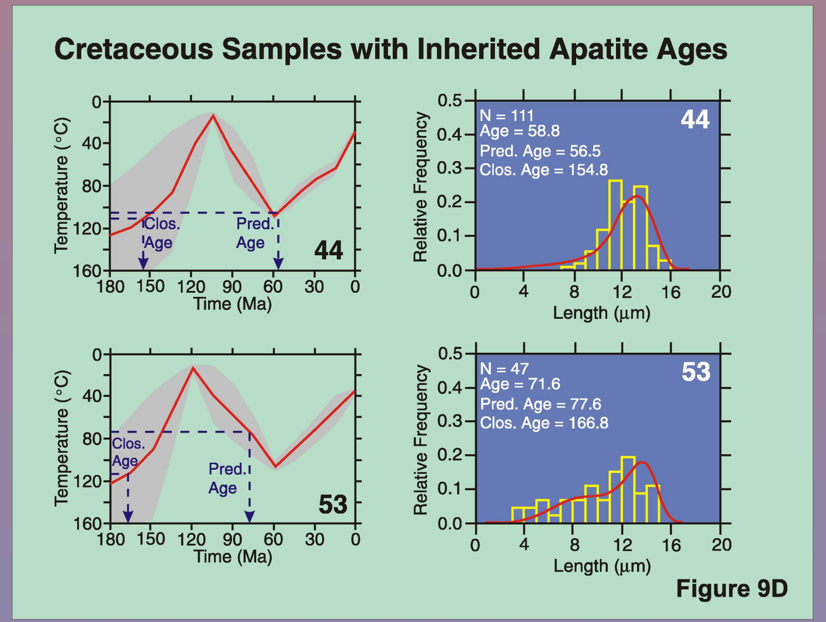

Figure 9D

Figure 9. A) Location of selected Cretaceous samples illustrative of volcanic-type samples and samples with inherited AFT ages. B) Ten Cretaceous samples (21, 55, 56, 57, 59, 79, 89, 97, 103, 105) have fission track ages that are slightly younger than their stratigraphic ages with corresponding track length distributions that have a relatively long mean length, small standard deviation and few short tracks. These characteristics, along with the observed low organic maturity (0.3-0.5%Ro), suggest that the detrital apatite in these samples may have been derived from a contemporaneous volcanic source at the time of deposition and that these samples experienced relatively little post-depositional annealing. Panel B shows temperature histories inferred for sample 59 for two sets of prior conditions: (a) Assumed volcanic source where apatite is formed effectively instantaneously at low temperature at the time of deposition of the sample; (b) Assumed detrital source where temperature is constrained to cool prior to the time of deposition of the sample with subsequent constraints being the same as in (a). Note that for both models (a) and (b), thermal histories following the time of deposition and the AFT length distributions are nearly identical. Therefore, the volcanic source model was used to model other samples having the same characteristics. C) Examples of thermal histories for volcanic-type Cretaceous AFT samples. D) The remaining Cretaceous samples have AFT age and length distributions which are inconsistent with a volcanic source model and instead were modelled using the pre-depositional thermal history constraints of model (b) (Fig. 9B). Example thermal histories are shown for samples 44 and 53.

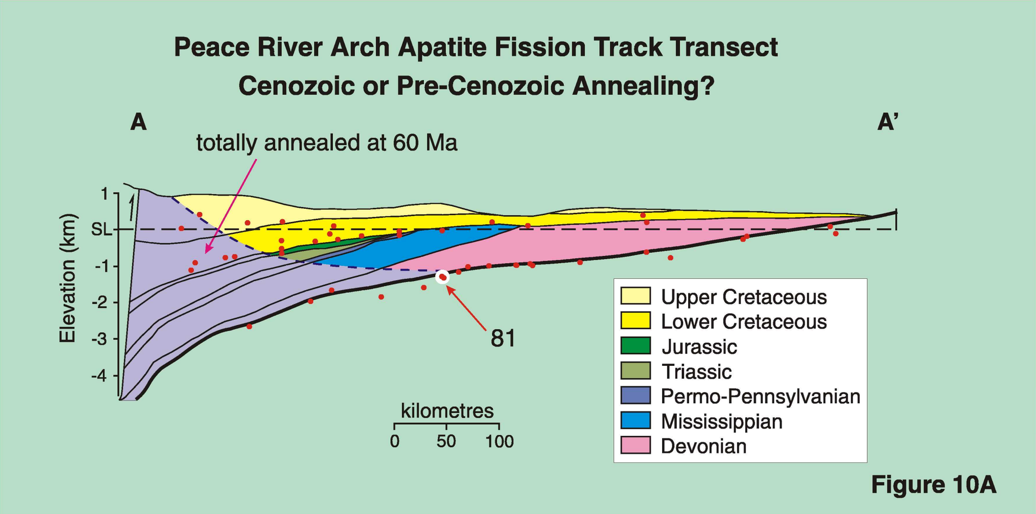

Figure 10A

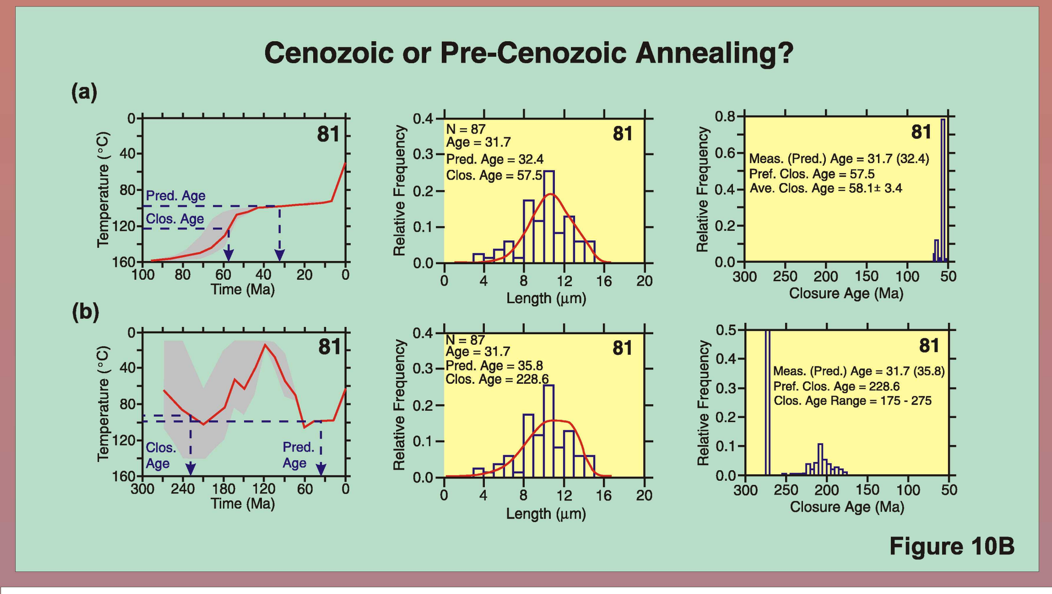

Figure 10B

Figure 10. A) Location of sample 81 which is illustrative of samples that can be fit by divergent thermal histories that do not allow for a unique interpretation. B) Thermal histories, track length distributions and closure age distributions for sample 81 assuming (a) complete annealing during the Cenozoic, and (b) pre-Cenozoic heating. The young AFT age suggests complete Cenozoic annealing but the large number of short tracks suggests a pre-Cenozoic history. We subjectively prefer model (B) because of the abundance of short tracks and because the estimated paleotemperatures are more consistent with those derived from sample 79 which directly overlies samples 81 and 82 in the same well.

Figure 11. Alternative interpretations of AFT paleotemperatures. A) Estimated pre-erosion surface position (symbols above cross section) from inferred maximum paleotemperatures at 60 Ma, assuming a constant paleogeothermal gradient of 30°C/km (present geothermal gradients vary between 25-30°C/km) and a paleosurface temperature of 10°C. Error bars for pre-erosion surface estimates are from the range in paleotemperature inferred from the AFT modelling. Also shown for reference is the Cenozoic paleosurface at maximum burial (green curve) estimated using coal moisture data (see Fig. 1). Paleotemperatures are shown next to the projected sample locations (red dots) on the cross section. This is not our preferred interpretation because the burial pattern inferred from the AFT data is not expected for a basin formed by flexural subsidence nor is the predicted deep burial in the east consistent with the high primary porosities of Lower Cretaceous sandstones in the east. B) Preferred interpretation. Estimated paleogeothermal gradients from inferred paleotemperatures at 60 Ma, calculated using a paleosurface temperature of 10°C and coal moisture-based estimates of maximum Cenozoic burial (see Fig. 1). Positions of the basement domains from Ross *et al*. (1991) (see Fig. 2) are shown above the line of section. C) Paleogeothermal gradient distribution at 60 Ma for the AFT transect of Ravenhurst *et al*. (1994) (see Fig. 1 for location). The dashed line shows the present geothermal gradient distribution. Note that paleogeothermal gradients are similar for both transects in their eastern parts (compare panels B and C) but that they differ by up to 20°C/km at their western ends.

Conclusions

1) Differentially annealed Cretaceous samples are younger than their stratigraphic age and, despite being detrital in nature, most of them show little evidence of a pre-depositional history. These observations, grain morphological criteria and other geological considerations indicate that most of the studied Cretaceous samples were derived from either a contemporaneous volcanic source at the time of deposition or from a rapidly exhumed igneous source.
2) Modelling of closure ages for fully annealed samples indicates that maximum paleotemperatures, and assumed maximum burial, were attained approximately at 60 Ma.
3) Maximum paleotemperatures, when combined with reconstructions of maximum burial, yield spatially and temporally variable paleogeothermal gradients. Paleogeothermal gradients along central portions of the PRA transect agree with present geothermal gradients (approximately 30°C/km) but are anomalously high with respect to present gradients at the eastern and western ends of the transect; paleogeothermal gradients of 35-40°C/km in the west and 35-60°C/km in the east. On the transect to the south, estimated paleogeothermal gradients in the westernmost part of the basin are as low as 50% (~20°C/km) of those estimated for the north. We interpret the paleotemperature data as reflecting thermal perturbations caused by large scale fluid flow near the end of the Laramide Orogeny in latest Paleocene time.
4) The anomalously high paleogeothermal gradients for the west end of the PRA transect overlie the Ksituan High but their relation to basement structure is unclear. The sedimentary section overlying the Arch is faulted and these faults may have acted as conduits for the upward movement of hot fluids.

REFERENCES

1) Hacquebard, 1977, *in* Deroo, G., Powell, T.G., Tissot, B. and McCrossan, R.G., (eds.), The Origin and Migration of Petroleum in the Western Canada Sedimentary Basin, Alberta - A Geochemical and Thermal Maturation Study, GSC Bull. 262, 11-22.
2) Issler, D.R., Beaumont, C., Willett, S.D., Donelick, R.A., Mooers, J. and Grist, A., 1990, Bull. Can. Petr. Geol., 38A, 250-269.
3) Nurkowski, J.R., 1984, AAPG Bull., 68, 285-295.
4) Ravenhurst, C.E., Willett, S.D.,Donelick, R.A. and Beaumont, C., 1994, J. Geophys. Res., 99, 20023-20041.
5) Ross, G.M., Parrish, R.R., Villeneuve, M.E. and Bowring, S.A., 1991, Can. J. Earth Sci., 28, 512-522.
6) Steiner, J., Williams, G.D. and Dickie, G.D., 1972, *in* Mellon, G.B., Kramers, J.W. and Seagel, E.J., (eds.), Proceedings, First Geological Conference on Western Canadian Coal: Edmonton, Res. Council of Alberta, Information Series no. 60, 85-96.
7) Willett, S.D., *submitted*, Inverse modelling of annealing of fission tracks in apatite 1; a controlled random search method. Am. J. Sci.
8) Willett, S.D and Issler, D.R., 1992, *in* Zentilli, M. and Reynolds, P.H., (eds.), Low Temperature Thermochronology, MAC Short Course Handbook, v. 20, 157-185.
9) Willett, S.D., Issler, D.R., Beaumont, C., Donelick, R.A. and Grist, A.M., *submitted*, Inverse modelling of annealing of fission tracks in apatite 2; application to the thermal history of the Peace River Arch region, Western Canada Sedimentary Basin, Am. J. Sci.
10) Willett, S., Issler, D., Grist, A. and Beaumont, C., 1992, *in* Ross, G.M., (ed.), Alberta Basement Transects Workshop (March 4-5), Workshop Report #28, LITHOPROBE Secretariat, University of British Columbia, 104-117.

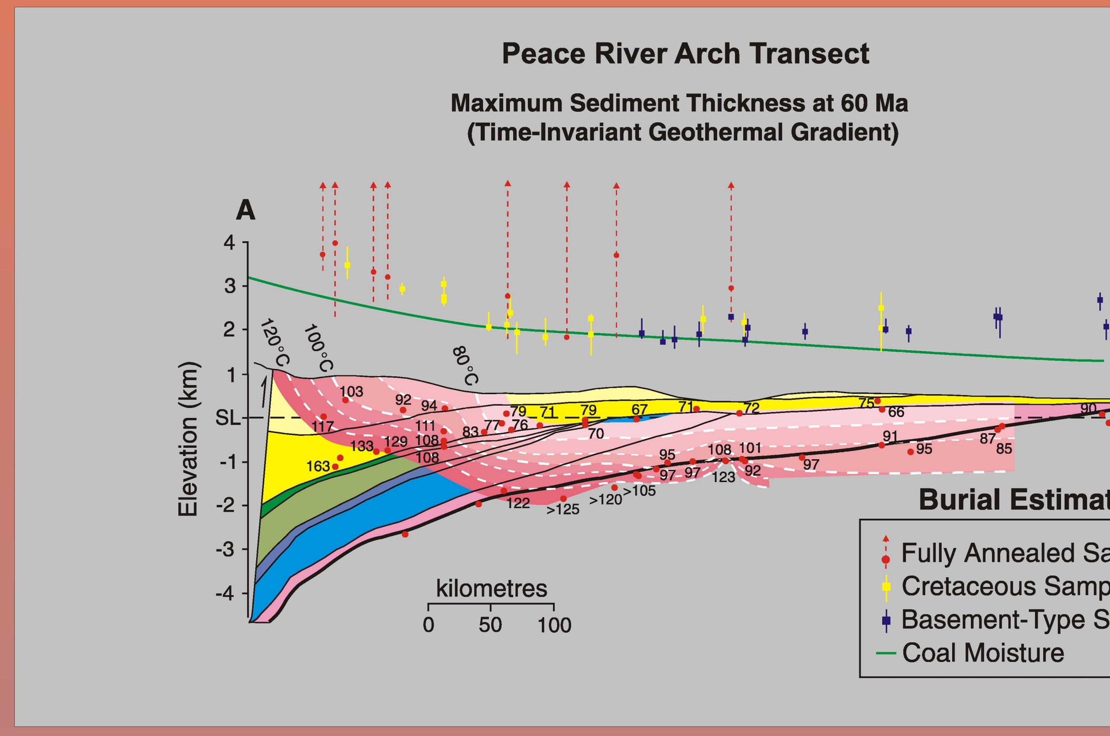

Figure 11A

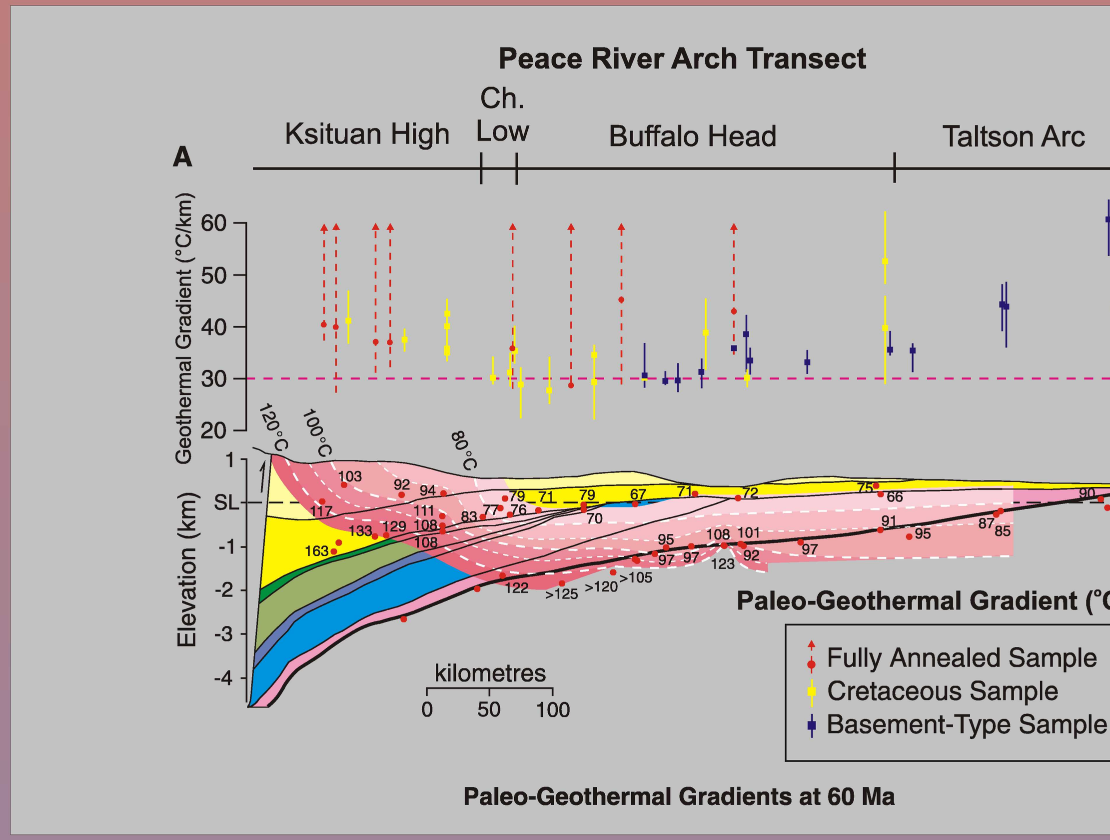

Figure 11B

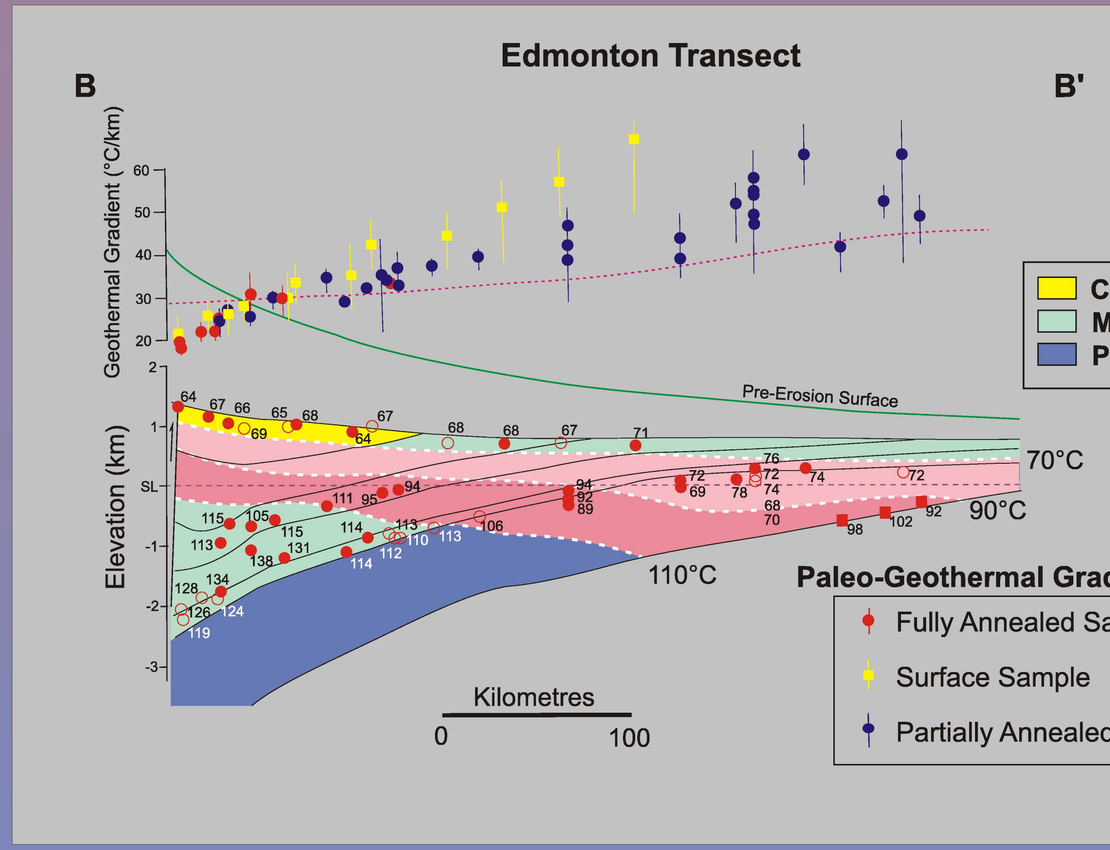

Figure 11C

Canada